Performance Analysis of Ball Mill Liner Based on DEM-FEM Coupling

Zhen Xu[1], Junfeng Sun[2*], Taohong Liao[3], Xiangping Hu[4*], Xuedong Zhang[5]

[1]Faculty of Mechanical and Electrical Engineering, Yunnan Open University, Kunming 650500, China

[2]Faculty of Mechanical and Electrical Engineering, Kunming University of Science and Technology, Kunming 650500, China

[3]Department of Marine Technology, Norwegian University of Science and Technology, Trondheim, Norway

[4]Industrial Ecology Programme, Department of Energy and Process Engineering, Norwegian University of Science and Technology, Trondheim, Norway

[5]SAIC Iveco Hongyan Commercial Vehicle Co., Ltd., Chongqing 401122, China

*Corresponding author: Junfeng Sun (sunjunfeng@kmust.edu.cn) and Xiangping Hu (Xiangping.Hu@ntnu.no)

Abstract. In the paper, based on the finite element-discrete element method coupling and the coupled bionics theory, four lifting bar models with coupled bionic surface structures, such as smooth, transverse stripe, longitudinal stripe and convex hull, are established. The particle model with different geometric features is established and the coupled simulations using finite element-discrete element method are carried out. Results show that the lift bar with the coupled bionic structure with soft matrix-hard bearing unit can effectively reduce the equivalent stress of the lifting bar during grinding. This coupled bionic structure can also reduce wear and tear of the lifting bar, and therefore, the lifting bar is protected and the grinding effect is improved. Results also indicate that the transverse stripe-coupled bionic structure has the best wear resistance and grinding effect comparing among the four kinds of lifting bars.

Keywords: ball mill; lifting bar; DEM-FEM; liner wear; equivalent stress; coupled bionic structure

1 Introduction

As an important equipment in the field of mineral processing, ball mills play crucial roles in normal operation of the national economy [1-3]. For ball mills, wear and tear of the lifting bars are the main causes of failure of the liner of the ball mill. According to historical data [4], wet ball mills consumed more than 110,000 tons of liners in metal mines during 2004 in China. However, green environmental protection is the mainstream trend of world economic development, which adds new requirements on equipment efficiency to save energy. Therefore, selecting a suitable wear-resistant material and designing a reasonable structure of the liner is of great importance for the ball mill.

2 Typical biological structure analyses

Two biological characteristics of the buttercup and the ostrich toe make them to have excellent wear and impact resistance [5]. These characteristics are closely related to the surface topography, hierarchy, and materials of the organism. The unit shape of the wear-resistant part of the ostrich toe is a spherical crown type convex body. This part of the toe is in contact with the ground and has a high frequency of

abrasive wear with sand. By measuring the cross section, it is found that the ratio of height, width and adjacent spacing of the bottom of the convex body is about 5:3:1. Similarly, the ratio of the intercostals grooves, rib width and rib height can be found from the surface morphology of the clam shell and it is about 4:3:1.

3 Lifting bar structure design

In this paper, the ball mill prototype with the cylinder size 600mm×400mm is used as the research platform, and the size of the incoming ore is 4mm-12mm. The proportional relationship discussed in Section 2 between the different parameters of the extracted biometrics is used to design the lifting bars with different characteristic surfaces. According to the relationship between the stripe and the direction of motion of the cylinder, the stripe is divided into horizontal stripe and vertical stripe. The three-dimensional model of the lifting bar with the stripe feature is shown in Figure 1. In the lift bar model, the width of the horizontal stripes and vertical stripes is M=6mm, the height is H=2mm, and the space between stripes is L=8mm. At the same time, according to the wear-resisting characteristics of ostrich toes, a lifting bar with convex features on the surface is designed. The unit of the convex hull feature has a diameter of M=6mm, a height of H=2mm, and the space between stripes is L=8mm. The designed lifting bar with convex hull feature is shown in Figure 2.

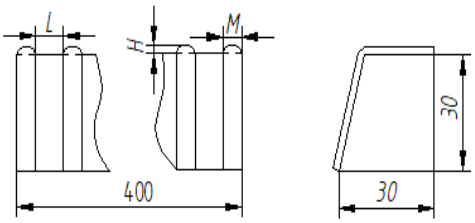

Fig.1 Lifting bar with stripe features

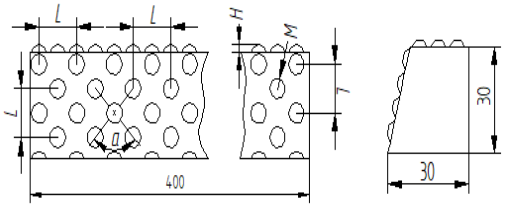

Fig.2 Lifting bar with convex hull feature

4 Simulation parameter definitions

The parameters of the mill in the simulation are as follows: the filling rate is 0.4 [6]; the diameter of the selected steel balls is 40 mm, 30 mm, 20 mm, and they match the medium using the equal number method. The material of the steel ball is ZGMn13, and the selected mill rotation rate is 65%.

4.1 Particle model establishment

The outlines of the particles are limited to spheres, tetrahedrons, hexahedrons, and diamonds. The mass distribution of particles and the shape in the simulation model are shown in Table 1.

Tab.1 The mass distribution of ore and grinding medium of each particle in the simulation

Particle size(mm)	Category	Shape	Quality(kg)
4	ore	sphere tetrahedron	8.568
7.5	ore	sphere tetrahedron Hexahedron diamond	11.424
12	ore	sphere tetrahedron	8.568

4.2 The meshing of geometry

Tetrahedral mesh is used for the liner, the lifting bar and its bionic unit. A single liner was analyzed when the amount of wear was counted.

4.3 Setting of simulation model

Set the motion of the geometric model to a linear rotation, and the speed is 35.55 rpm. The geometric model starts from 1.45s, and the total simulation time is 2.9s. The motion of materials in the ball mill at different time points are shown in Figure 3, where Figure 3 (a) shows the static accumulation state after blanking is completed, and Figure 3 (b) shows the motion state of the material at 2.9s.

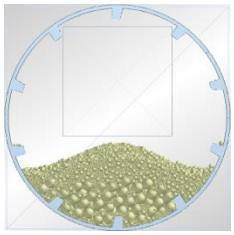

(a)Static accumulation state after blanking

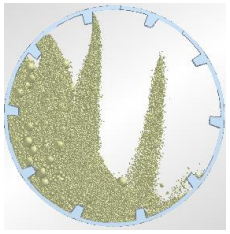

(b)The motion state of the material at 2.9s

Fig.3 The motion of materials in the ball mill at different time points

5 Simulation result analysis

The static analysis of the liner is based on the DEM-FEM coupling method. The force obtained in EDEM and its simulation files are imported into the EDEM module. Therefore, the meshing in the coupling analysis is consistent with the discrete element simulation. In such a way that a more accurate solution can be obtained.

The wear of the lifting bar is related to the impact of the material and the medium on the lifting surface. Therefore, the equivalent stress distribution on the surface of the lifting bar are analyzed in detail. Figure 4 to Figure 7 show the equivalent stress distribution of the ball mill cylinder model with four different surface feature lifting bars in a certain period. Results in Figure 4 illustrate that the smooth surface of lifting bar is most concentrated in the joint portion of the lifting bar and the substrate of liner during a certain period of mill operation. Secondly, Stress concentration occurs at the adjacent part of the surface of lifting bar and the upper surface. This is because the contacts between the material and the medium in these places are the severest, and it is known that the stresses at both ends of the lifting bar are also higher than the stress in the middle of the bar. It can be seen from Figure 5 that the equivalent stress on the surface of the lateral stripe surfacing feature lift bar is mainly concentrated in the adjacent part of the lift bar and the liner base, and there is no obvious stress concentration. The stress between the bionic features is lower than that of the bionic features. From the stress and its distribution, the value is smaller than that of the smooth surface features.

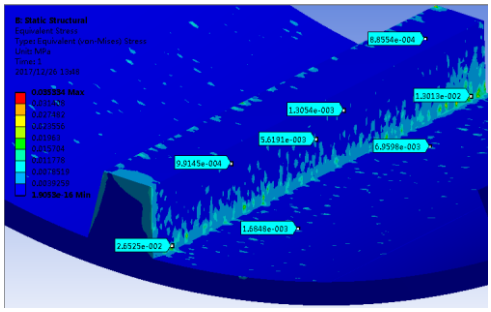

Fig.4 Equivalent stress distributions of smooth surface lifting bars and its surrounding area

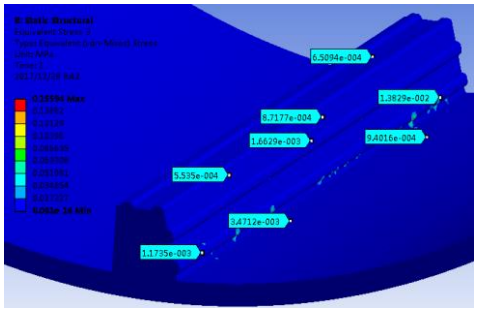

Fig.5 Equivalent stress distributions of horizontal stripes surface lifting bars

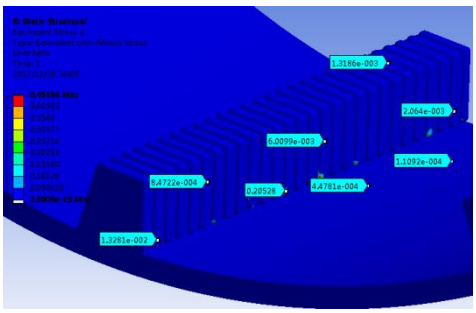

Fig.6 Equivalent stress distributions of vertical stripes lifting bars

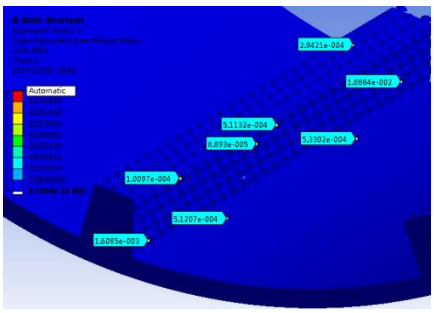

Fig.7 Equivalent stress distributions of convex hull lifting bars

Figure 6 shows the stress distribution of the lifting bar of the longitudinal stripe feature. The stress is mainly distributed at the end of the longitudinal feature of lifting bar and near the substrate of the liner. This is related to the geometric dimension of the end of the feature and the size of the material. Since the particles stay between the bionic feature and the substrate of the liner, the stress becomes larger. In general, the stress value of the longitudinal feature of lifting bar is smaller than that of the smooth surface. In Figure 7, the distribution of overall stress is uniform compared to the other three lift bars. At the same time, the stress value on the feature unit is smaller than the stress value of the lateral feature bar. These results show that the stress relieving effect of the convex hull type bionic feature is better than other bionic feature in the simulation. However, on the matrix between the features, there is few difference between the vertical stripes lifting bar and even the smooth surface lifting bar, so that the protection effect on the substrate is limited. To make a more accurate study of the wear zone distribution of each lifting bar during the grinding process, the EDEM post-processing module is used to select the "Geometry Bin" option. The concentrated area of the liner and lifting bars are divided into two parts, and the areas are numbered and shown in Figure 8.

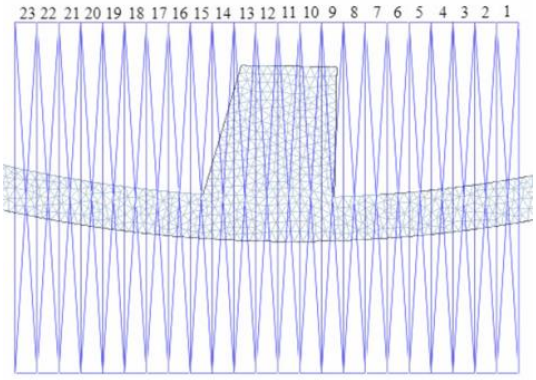

Fig.8 The divided area of the liner and the lifting bars

In the post-processing module of EDEM, the "Arc hard Wear" option in the geometry section is selected in "File Export-Result Date", since this option evaluates the amount of wear based on the accumulated energy. The trend can also verify the cumulative energy received by the liner and the lifting bar in this simulation. The accumulated energy received by the liner and the lifting bar is plotted after the ball mill model with different surface feature operated for a period, and this result can be used to intuitively compare the amount of wear in the same area. The relationship is shown in Figure 9.

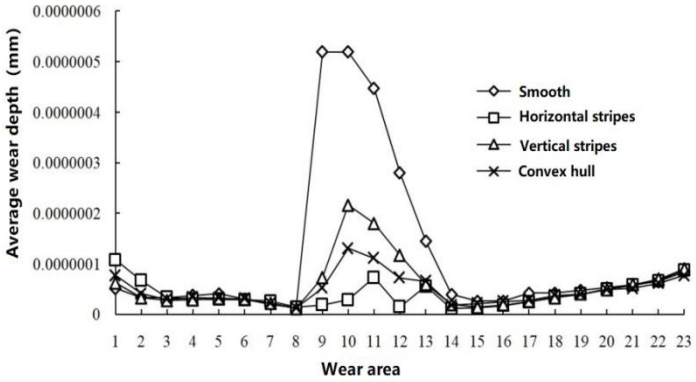

Fig.9 The wear distribution of specified area in different liner and lifting bars

As shown in Figure 9, for the liner where the smooth surface feature lifting bar is mounted, the main wear position is located between the upper surface of the lifting bar and the non-lifting surface, i.e., between the region 9 and the region 14. The amount of wear in the region 9 is 5.19E-7mm. This is because of the right-angled trapezoidal liner used in this simulation. Therefore, stress concentration appears at the common edge of the non-lifting surface (region 9) and the upper surface. At the same time, the transition region between the upper surface and the lifting surface (region 13) undergoes relatively intense friction during the grinding process with the material raised to the highest point, and this is the reason why the amount of wear is correspondingly high. The reason why the amount of wear of the area 10 to area 12 is also relatively large is that from the time when the upper surface is in contact with the material, and the time when the material begins to drop, the material does more work for the location than the work done on the lifting surface, so the amount of wear is slightly larger than the area 13 to area 15. The wears of other areas are significantly lower than the ones in area 9 to area 14.

6 Conclusions

In this paper, the stress distribution of the lifting bar and its surrounding area during the grinding process is analyzed. At the same time, the wear areas of the lifting bar of different surface features are compared. The results are summarized as follows:

(1) During the grinding process, the stress of the lifting bar is mainly concentrated in the adjacent part of the lifting bar and the liner, and the values in the two ends are larger than the one in intermediate part. The smooth surface lifting bar has obvious stress concentration during the grinding process, and the concentrated area is the widest among the four lifting bars. The stress relaxation effect occurs in all three different bionic feature units, and this reduces the equivalent stress of the lifting bar to a certain extent and improves the wear resistance of the lifting bar.

(2) Although the stress on the convex hull type bionic feature unit is significantly reduced, the effect of the release of the equivalent stress on the lifting bar base is lower than that of the horizontal stripe. The order of the stress relieving effect of the bionic feature unit, from high to low, is horizontal stripe, convex hull feature and vertical stripe.

(3) During the grinding process, the wear of the liner surface and the lifting surface of the right angle trapezoidal lifting bar is significantly higher than that of the liner between the lifting bar, and the most severely worn area are mainly concentrated near the common side of upper surface and lifting surface.

(4) Comparing with the lifting bar on the smooth surface, the liner with the bionic feature lifting bar has better wear resistance, and the order of the wear resistance of the liner, from low to high, is horizontal stripes, vertical stripes, and convex hull.

(5) The horizontal stripes bionic feature lifting bar can extend the replacement period of the mill liner and avoid the mill downtime caused by the inconsistent replacement period between the liner and the lifting bar. It can also reduce the number of liner replacements and extend the liner life cycle.

Acknowledgement

The work was fully supported by the Youth Project of Science and Technology Department of Yunnan Province (No.2017FD132). We gratefully acknowledge the relevant organizations.

References

1. Zhao Min, Lu Yaping, Pan Yingmin. Review on the theory of pulverization and the development of pulverizing equipment. Mining and Metallurgy, 2001, 10(2): 36-41

2. Zhang Guowang. Current status and development of crushing and grinding equipment. Powder technology. 1998, 4(3): 37-42

3. Belov, Brandt. Grinding. Liaoning: Liaoning People's Publishing House, 1954

4. Li Wei, Market and Production of Wear-resistant Steel Parts, Proceedings of the Annual Meeting of Yunnan Wear-Resistant and Corrosion-Resistant Materials, 2004. Kunming 7-12, 2004

5. Cao Zhanwang, Wang Dapeng, Ganxi. Research progress of Marsh's mother-of-pearl and seawater pearls. Journal of Southern Agricultural Sciences, 2009, 40(12): 1618-1622

6. Zhang Xuedong, Dong Weimin, Zhou Haiyan, et al. Numerical simulation of wear resistance of ball mill lifting bars with biomimetic characteristics. Nonferrous Metals (Mineral Processing), 2017(6): 56-62